Cis- and *trans*-membrane interactions of synaptotagmin-1

Wensi Vennekate[a,b], Sabrina Schröder[a], Chao-Chen Lin[a,b], Geert van den Bogaart[b], Matthias Grunwald[a], Reinhard Jahn[b,1], and Peter Jomo Walla[a,c,1]

[a]Research Group Biomolecular Spectroscopy and Single-Molecule Detection and [b]Department of Neurobiology, Max Planck Institute for Biophysical Chemistry, 37077 Göttingen, Germany; and [c]Department of Biophysical Chemistry, Institute for Physical and Theoretical Chemistry, University of Braunschweig, 38106 Braunschweig, Germany

Edited by Axel T. Brunger, Stanford University, Stanford, CA, and approved May 23, 2012 (received for review October 7, 2011)

In neurotransmission synaptotagmin-1 tethers synaptic vesicles to the presynaptic plasma membrane by binding to acidic membrane lipids and SNAREs and promotes rapid SNARE-mediated fusion upon Ca^{2+} triggering. However, recent studies suggested that upon membrane contact synaptotagmin may not only bind *in trans* to the target membrane but also *in cis* to its own membrane. Using a sensitive membrane tethering assay we have now dissected the structural requirements and concentration ranges for Ca^{2+}-dependent and -independent *cis*-binding and *trans*-tethering in the presence and absence of acidic phospholipids and SNAREs. Using variants of membrane-anchored synaptotagmin in which the Ca^{2+}-binding sites in the C2 domains and a basic cluster involved in membrane binding were disrupted we show that Ca^{2+}-dependent *cis*-binding prevents *trans*-interactions if the *cis*-membrane contains 12–20% anionic phospholipids. Similarly, no *trans*-interactions were observable using soluble C2AB-domain fragments at comparable concentrations. At saturating concentrations, however, tethering was observed with soluble C2AB domains, probably due to crowding on the vesicle surface and competition for binding sites. We conclude that *trans*-interactions of synaptotagmin considered to be essential for its function are controlled by a delicate balance between *cis*- and *trans*-binding, which may play an important modulatory role in synaptic transmission.

neurobiology | two-photon | fluorescence correlation spectroscopy | fluorescence cross-correlation spectroscopy | docking

Upon arrival of an action potential, Ca^{2+} channels in the synaptic membrane open and increase local cytoplasmic Ca^{2+}. This increase is sensed by synaptotagmin-1, a 65-kDa protein anchored to synaptic vesicles (1, 2). Synaptotagmin-1 then triggers fusion of the synaptic vesicles with the plasma membrane resulting in release of neurotransmitter. Fusion itself is mediated by the vesicular R-SNARE synaptobrevin-2 and the plasma membrane Q-SNAREs SNAP-25 and syntaxin-1A. These SNAREs assemble *in trans* between the membranes and form a tight coiled-coil complex which overcomes the energy barrier of membrane fusion. Synaptotagmin-1 consists of an N-terminal transmembrane helix connected by a long (61-residue) unstructured linker to two C2 domains, called C2A and C2B. The C2A and C2B domains bind three and two Ca^{2+} ions, respectively (3, 4). They also bind to both individual Q-SNAREs and assembled SNARE complexes (1, 5–7) and to anionic membranes (3, 8–16). Both of these interactions are modulated by Ca^{2+} and have been implicated in the mechanism of synaptotagmin-1 action (1, 2). In addition, synaptotagmin-1 possesses a polybasic stretch in the C2B domain that is structurally separated from the calcium-binding domain and that mediates calcium-independent binding to acidic phospholipids, particularly phosphatidylinositol-4,5-bisphosphate (PiP_2) (8, 9, 15–17).

Despite intense research over the past two decades, it is still unclear by which molecular mechanism synaptotagmin-1 is capable of accelerating exocytosis by more than four orders of magnitude (18). Two types of models are presently discussed that are not necessarily exclusive. The first proposes a direct action of synaptotagmin-1 on the primed state of the fusion apparatus that is established before the arrival of the calcium trigger (3, 4, 19). This state is characterized by partially assembled *trans*-SNARE complexes in which further zippering is arrested, possibly involving binding of proteins such as complexin or synaptotagmin. Upon activation by calcium ions, synaptotagmin-1 may promote fusion by one of the following mechanisms (20): (*i*) binding to the SNAREs and thus activating C-terminal zippering, possibly associated with displacement of complexin (activator model); (*ii*) dissociating from the SNARE complex, thus relieving arrest of SNARE zippering (fusion clamp model); and/or (*iii*) binding to the lipid bilayer close to the membrane contact site. The latter may destabilize the membrane or induce curvature, thus lowering the energy barrier for fusion. The second model proposes a tethering/docking role of synaptotagmin-1, mediated by "*trans*" binding to acidic phospholipids in the plasma membrane and/or direct binding to the Q-SNAREs. According to this scenario, calcium activation may result in a closer connection between the vesicle and the plasma membrane that promotes fusion, for instance by facilitating SNARE assembly which is the rate-limiting step in fusion (17).

To shed light on the molecular mechanism of synaptotagmin-1, SNARE-mediated fusion has been reconstituted in liposomes. Both stimulatory and inhibitory effects by synaptotagmin-1 on fusion were reported. In several studies, acceleration was attributed to a tethering/docking function of synaptotagmin-1, which promotes SNARE zippering (19, 21). However, tethering is usually not measured separately, thus a decisive intermediate is not observed. Further complications arise from the observation that membrane-anchored synaptotagmin-1 may bind to its own membrane once activated by calcium (*cis*-binding). Because *cis*-binding may compete with membrane tethering (22, 23) it seems likely that this poorly understood phenomenon—which may play an important modulatory role in synaptic transmission—is responsible for the enormous differences in Ca^{2+} sensitivities of synaptotagmin-1–triggered membrane fusion among various in vitro studies, which can range from as low as 10 μM (24) to higher than 3 mM Ca^{2+} (25).

In the present study, we have systematically investigated *cis*- and *trans*-binding activities of membrane-anchored synaptotagmin using conditions where no fusion occurs. Previous work has shown that membrane binding *in trans* by synaptotagmin-1 is strong enough to tether membranes. Clustering of liposomes by

Author contributions: R.J. and P.J.W. designed research; W.V., S.S., and C.-C.L. performed research; G.v.d.B. and M.G. contributed new reagents/analytic tools; W.V., S.S., and C.-C.L. analyzed data; and W.V., G.v.d.B., R.J., and P.J.W. wrote the paper.

The authors declare no conflict of interest.

This article is a PNAS Direct Submission.

Freely available online through the PNAS open access option.

[1]To whom correspondence may be addressed. E-mail: rjahn@gwdg.de or pwalla@gwdg.de.

This article contains supporting information online at www.pnas.org/lookup/suppl/doi:10.1073/pnas.1116326109/-/DCSupplemental.

synaptotagmin was observed using dynamic light scattering (DLS) (10, 17) or turbidity measurements (22). However, due to the limited sensitivity of these assays tethering can only be observed when clusters consisting of multiple liposomes are formed. Therefore, we used two-photon fluorescence cross-correlation spectroscopy (TP-FCCS) (23, 26), which is sufficiently sensitive to report tethering between two individual liposomes and can easily be quantified. TP-FCCS is based on analyzing fluorescence fluctuations caused by diffusion of fluorescently labeled liposomes through a two-photon excitation volume (dimension ~200–500 nm). It is ideally suited to quantify the proportion of free and docked liposomes (for details see Fig. S1 and ref. 23). Autocorrelation analysis of labeled liposomes directly provides their average number in the excitation volume. Cross-correlation of differently labeled liposomes is a direct measure for the proportion of tethered liposomes in the total liposome population. Thus, with TP-FCCS, detailed information about membrane tethering by synaptotagmin-1 can be obtained within a few seconds of measuring time and immediately after initiating tethering by mixing, thus avoiding artifacts such as slow nonspecific aggregation.

Results

To analyze the ability of membrane-anchored synaptotagmin-1 to tether membranes, we reconstituted full-length recombinant synaptotagmin-1 into liposomes and measured tethering to protein-free liposomes using TP-FCCS. In addition to wild-type synaptotagmin-1, we used point mutants (C2a*B, C2Ab*, and C2a*b*) in which calcium binding to either one or both C2 domains was disrupted (C2a*B: D178A D230A D232A; C2Ab*: D309A D363A D365A; C2a*b*: D178A, D230A, D232A, D309A, D363A, and D365A) (3) and mutations in which the polybasic stretch of the C2B domain was inactivated (K326A, K327A; KAKA mutant). Synaptotagmin-1 was incorporated at 1:1,000 molar protein-to-lipid ratio into liposomes that were labeled with 1 mol% Texas red-DHPE, whereas the protein-free target liposomes were labeled by using 1.5 mol% of all lipids Oregon green-DHPE. Unless indicated otherwise, target liposomes contained acidic phospholipids (20% of all lipids were phosphatidylserine) (PS) (for more details see Table S1).

In the first set of experiments (Fig. 1*A*), the synaptotagmin-1 bearing liposomes were free of acidic phospholipids to exclude *cis*-binding. Under these conditions, moderate tethering was observed that was enhanced more than twofold upon addition of 100 μM Ca^{2+} (red bars in Fig. 1*A*) and reverted when Ca^{2+} was chelated with 500 μM EGTA (<5% tethering). A total of 1 mM Mg^{2+} did not influence membrane tethering. Tethering was dependent on synaptotagmin-1 because no tethering was observed without synaptotagmin-1 (control in Fig. 1) or with an inactive mutant in which Ca^{2+} binding in both C2 domains as well as the polybasic stretch was inactivated (<5% tethering in all cases). We can safely exclude membrane fusion under any of the conditions tested in this work, because membrane fusion would result in Förster resonance energy transfer and decreased lifetimes of Oregon green-DHPE (23), which was not observed.

Upon disruption of Ca^{2+} binding of either the C2A or the C2B domain still a maximum tethering as with wild-type synaptotagmin-1 was observed in the presence of 100 μM Ca^{2+} (a*B and Ab* in Fig. 1*A*). However, when the Ca^{2+} concentration was reduced (8.5 μM Ca^{2+}), the tethering activity of both mutants was lower (about 10–20% above the level of no Ca^{2+}, Fig. S2*B*, red lines). When both Ca^{2+}-binding domains were disrupted, no Ca^{2+}-dependent enhancement of tethering was observable (C2a*b* in Fig. 1*A*) even when the Ca^{2+} concentration was increased to 880 μM in agreement with previous observations (17, 22) (see also Fig. S2*B*, black line). Calcium-independent tethering is mediated by the polybasic lysine patch on the C2B domain (10, 17), because removal of charges (KAKA mutant)

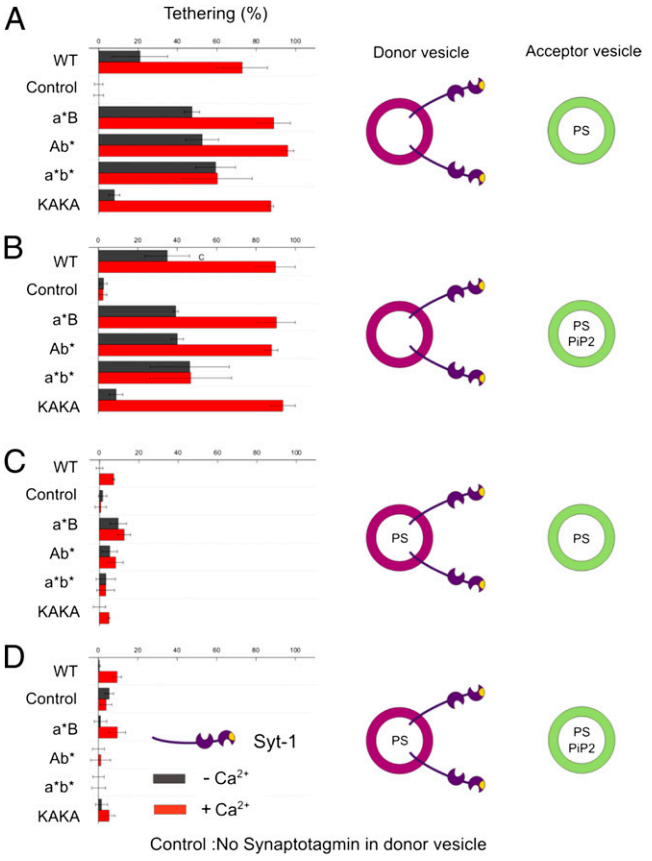

Fig. 1. Tethering of liposomes mediated by membrane-bound synaptotagmin-1. The fraction of green acceptor liposomes tethered to red donor liposomes reconstituted with recombinant full-length synaptotagmin-1 was determined with TP-FCCS in the presence (red bars) or absence (black bars) of Ca^{2+} (100 μM final concentration, see Fig. S1 for more details). Acceptor liposomes contained 20% PS and (if indicated) 1% PIP_2. Donor liposomes contained either no PS (*A* and *B*) or 20% PS (*C* and *D*). In the control, no synaptotagmin was present in the vesicles. (*A*) Tethering between donor liposomes reconstituted with synaptotagmin variants [wild type (WT), C2a*B, C2Ab*, C2a*b*, KAKA] and acceptor liposomes. Donor liposomes were free of acidic phospholipids, whereas acceptor liposomes contained 20% phosphatidylserine (PS). (*B*) Same as *A* but 1% PiP_2 was included in the membrane of the target liposomes. (*C* and *D*) Same as in *A* and *B* but with 20% PS included in the membrane of the donor liposomes.

virtually abolished tethering while Ca^{2+}-dependent tethering remained unaffected (KAKA in Fig. 1*A*).

To investigate whether the presence of PiP_2 enhances tethering, the experiments described above were repeated using target liposomes that, in addition to 20% PS, also contained 1 mol% PiP_2 (Fig. 1*B*). No major tethering differences were observed when using no or 100 μM Ca^{2+}. This finding is not surprising because already full tethering is observed even without PiP_2 in the presence of 100 μM Ca^{2+} (Fig. 1*A*). However, at reduced Ca^{2+} concentrations (~8.5 μM) more tethering was observed with the mutants C2a*B and C2Ab* when PiP_2 was present in the target membrane (Fig. S2*B*, green lines).

To examine whether binding of synaptotagmin-1 to its own membrane affects its tethering activity, the experiments were repeated using synaptotagmin-1–bearing liposomes containing 20% PS (Fig. 1 *C* and *D*). Most strikingly, the presence of PS almost completely prevented membrane tethering in all conditions, regardless of whether the target membrane contains PS only or PS plus PiP_2. Very similar observations were made when 12% PS was used, a concentration corresponding to that of

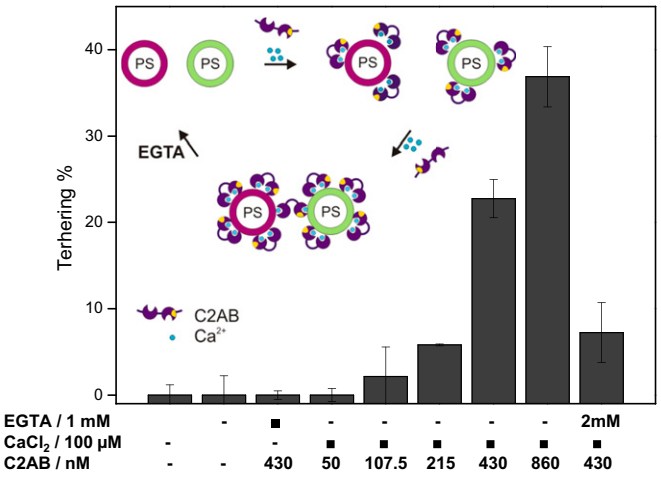

Fig. 2. Tethering of liposomes mediated by soluble C2AB domains of synaptotagmin-1. Ca^{2+} -dependent tethering was only observable when soluble C2AB fragments were added at concentrations above 200 nM. See Fig. 1 legend, *SI Methods*, and Fig. S1 for more details.

native synaptic vesicles (Fig. S3*A*). When the PS concentration in the synaptotagmin-1–bearing liposomes was reduced to 5% PS, Ca^{2+}-dependent tethering was restored approximately to the level of liposomes containing no PS (Fig. S3*B*), whereas Ca^{2+}-independent tethering, mediated by the polybasic patch, was still inhibited unless PiP_2 was present in the target membrane.

These results were unexpected because soluble C2AB domains were shown previously to cluster liposomes containing acidic phospholipids in the presence of calcium (10, 17, 22). Thus, it is conceivable that membrane anchorage restricts the mobility of the C2 domains in such a way that upon *cis*-binding there are no free binding sites available that allow for *trans*-binding. To shed light on this issue, we carried out tethering experiments using a soluble fragment of synaptotagmin-1 containing the C2AB domains (residues 97–421). Intriguingly, Ca^{2+}-dependent tethering was only observable when the C2AB fragment was added at elevated concentrations (above 200 nM, Fig. 2), whereas virtually no tethering (approximately 4%) was observed at a concentration of 50 nM [comparable to that of the membrane-anchored version (43–120 nM)] even if the incubation time was extended to 30 min. All tethering was reversed upon adding 1–2 mM EGTA (Fig. 2).

It is conceivable that under our experimental conditions a concentration of 50 nM soluble C2AB domain is too low to result in membrane binding upon addition of Ca^{2+}, thus explaining the absence of tethering under these conditions. To find out which C2AB-concentration is necessary for membrane binding, we performed a set of experiments in which Alexa 488-labeled C2AB domains (AF-C2AB) were added to solutions of red liposomes containing 20% PS (Fig. 3*A*). These experiments revealed that soluble AF-C2AB domains bind with high efficiency at concentrations of 50 nM as well as 215 nM to the membranes even though tethering only began to be observable at concentrations above 215 nM (Fig. 2). Again, binding was reverted by adding 1 mM EGTA.

The discrepancy between Ca^{2+}-dependent binding and tethering prompted us to investigate whether saturation of binding needs to be achieved for tethering to become apparent. Fluorescence correlation spectroscopy (FCS) is capable of monitoring free and bound AF-C2AB separately, allowing us to address this question directly (Fig. 3*B*). Whereas at 50 nM AF-C2AB a very large fraction of all protein is bound to the liposomes in the presence of Ca^{2+}, the bound fraction drops significantly at 215 nM, suggesting that binding begins to saturate around this concentration. For further confirmation, we added increasing amounts of unlabeled C2AB domain to the labeled variant AF-C2AB (which was kept at 50 nM for these experiments). Whereas addition of 150 nM only resulted in a slight competition, addition of 400 nM of unlabeled C2AB caused substantial competition, with the fraction of bound labeled AF-C2AB dropping below

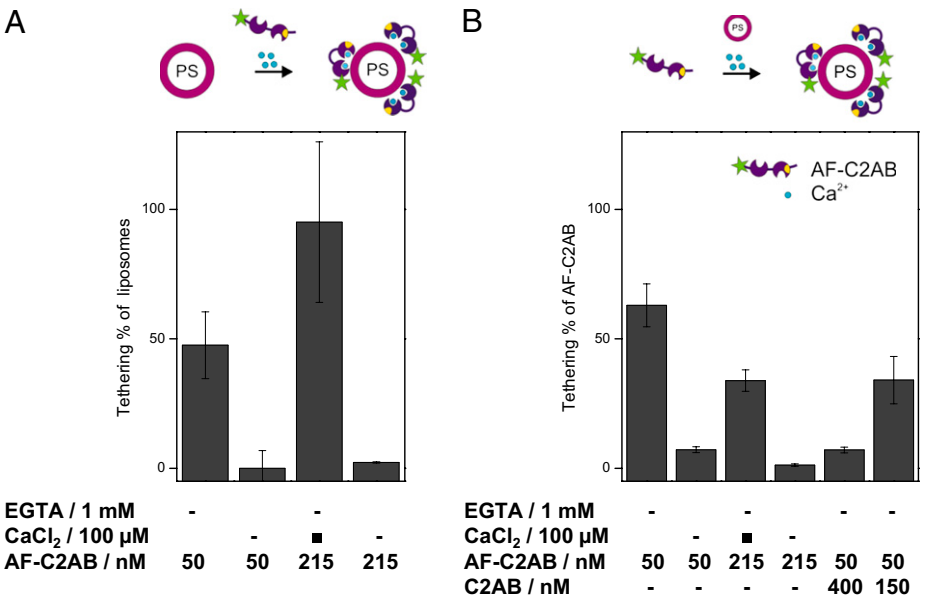

Fig. 3. Binding of soluble C2AB domains of synaptotagmin-1 to liposomes containing 20% PS. Soluble C2AB domains of synaptotagmin-1, labeled with Alexa 488 (AF-C2AB), were incubated with 10 nM liposomes containing 20% PS. Both free and bound C2AB and liposomes were determined by TP-FCCS. (*A*) Percentage of liposomes containing bound C2AB domains. At C2AB concentrations of 215 nM all liposomes contained bound C2AB. Binding was prevented by EGTA. (*B*) Extent of soluble C2AB domains bound to liposomes. When the total concentration of labeled (AF-C2AB) and unlabeled C2AB fragments exceed 215 nM the bound fraction drops significantly, suggesting that binding begins to saturate around this concentration. Again, binding was prevented by EGTA.

10% (Fig. 3*B*, columns 5 and 6). We conclude that liposome tethering or clustering effected by soluble C2AB domains in the presence of Ca^{2+} requires saturation of the membrane surface with C2AB domains (*Discussion*).

In the final set of experiments, we investigated liposome tethering by binding of membrane-anchored synaptotagmin-1 to SNAREs (1, 5–7) (Fig. 4). To rule out *trans*-binding to acidic phospholipids, the SNAREs were reconstituted into liposomes lacking acidic phospholipids. Efficient tethering was observed when target liposomes containing either syntaxin-1A (183–288) alone (Sx1A), a binary Syntaxin 1A-SNAP-25 complex (Sx1A-SN25) or a fully assembled ternary complex consisting of synaptobrevin 2 (1–96), SNAP-25, and syntaxin 1A (Sx1A-SN25-Sb2) were used (Fig. 4*A*). This tethering was significantly larger than tethering mediated by SNARE proteins in the absence of synaptotagmin (Fig. 4*B*). Binding was also not due to nonspecific adsorption because it was not prevented by adding 10 mg l^{-1} BSA. Addition of Ca^{2+} did not result in a further enhancement except of a moderate enhancement when only syntaxin was used as target, in agreement with previous reports showing that the interaction between these two proteins is enhanced by calcium. Again, membrane tethering was completely prevented when 20% PS was present in the membrane of the synaptotagmin liposomes (Fig. 4*C*).

Because most of the observed tethering is Ca^{2+} independent the question arises whether the polybasic region of the C2B domain is required for such clustering. Therefore, we repeated the experiments using the KAKA mutant in which this region is disrupted (Fig. 4 *D* and *E*). Intriguingly, both basal and Ca^{2+} enhancement of tethering was preserved when target liposomes containing free syntaxin were used, whereas binding to both binary and ternary SNARE complexes was reduced to background levels. Again, the observed tethering to free syntaxin was reduced significantly when the synaptotagmin-1 liposomes contained 20% PS.

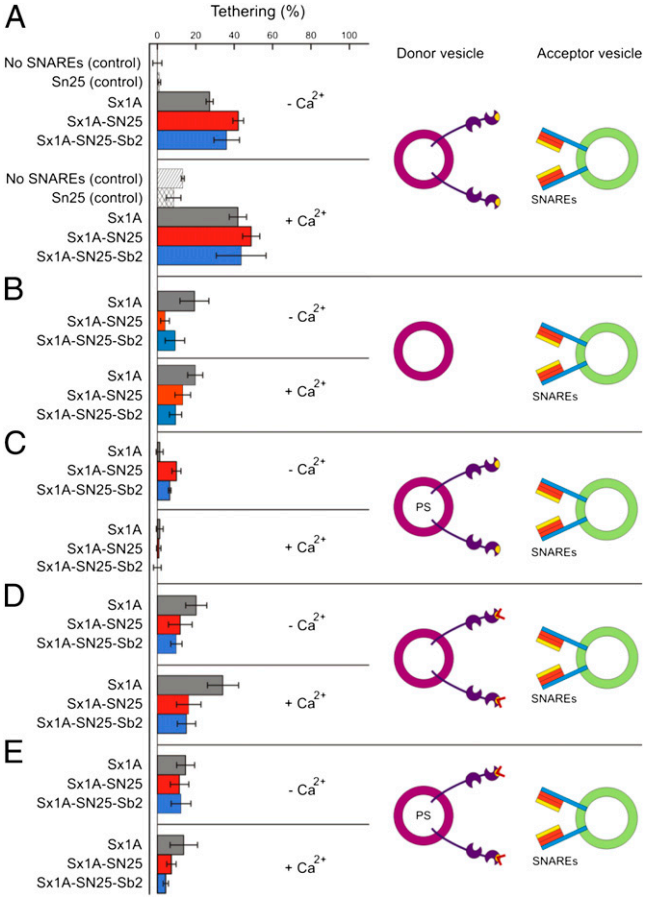

Fig. 4. Tethering of liposomes mediated by synaptotagmin–SNARE interactions. Acceptor liposomes devoid of acidic phospholipids were reconstituted with purified recombinant syntaxin-1A (Sx1A; gray); a binary complex of syntaxin-1A and SNAP-25 (Sx1A-SN25; red), or a ternary SNARE complex (Sx1A-SN25-Sb2; blue) at a 1:1,000 molar protein-to-lipid ratio. Control incubations involved acceptor liposomes without SNAREs or only the presence of soluble SNAP-25. Incubations were carried out in the absence ($-Ca^{2+}$) or presence ($+Ca^{2+}$) of 100 μM Ca^{2+}. (*A*) Donor liposomes contained wild-type synaptotagmin-1 and were free of acidic phospholipids to prevent cis-binding. (*B*) Same as *A* but using donor liposomes containing no synaptotagmin as control. (*C*) Same as *A* but using donor liposomes containing 20% PS. (*D*) Same as *A* but using the KAKA mutant of synaptotagmin. (*E*) Same as *C* but using donor liposomes containing 20% PS.

Discussion

Using a sensitive liposome tethering assay based on TP-FCCS we have dissected the contributions of three independent membrane binding sites of synaptotagmin-1, two of which being regulated by Ca^{2+}, to synaptotagmin-1–mediated tethering of membranes. Several conclusions can be drawn from our study (Fig. 5). First, membrane-anchored synaptotagmin-1 binds to target membranes involving all three binding sites, generally confirming numerous previous reports addressing the membrane-binding properties of isolated C2 domain fragments (3, 9, 10). In the absence of Ca^{2+}, moderate *trans*-tethering by the basic cluster occurs. Full tethering by any C2 domain was observed in the presence of 100 μM Ca^{2+}. At around 8.5 μM Ca^{2+} full tethering

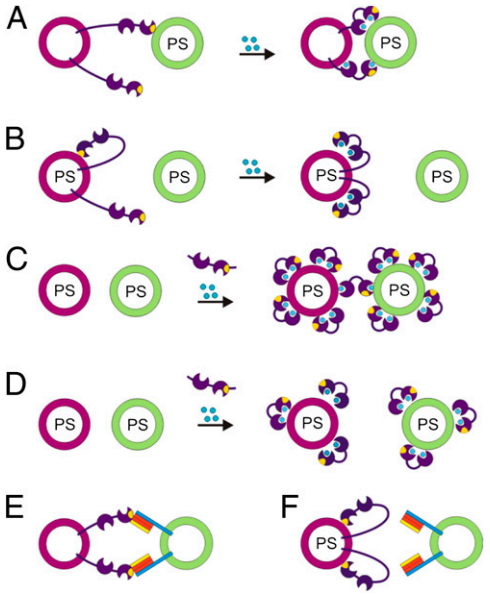

Fig. 5. Diagram summarizing how *cis*- and *trans*-membrane interactions of synaptotagmin determine membrane tethering. (*A*) In the absence of anionic lipids in the donor membrane, synaptotagmin binds *in trans* to an acceptor membrane containing phosphatidylserine (PS) involving both Ca^{2+}-independent (via the basic patch) and Ca^{2+}-dependent interactions. Blue circles symbolize Ca^{2+}. (*B*) *Cis*-binding dominates over *trans*-tethering if the donor membrane contains 20% PS, regardless of whether Ca^{2+} is added or PiP_2 is present in the target membrane. (*C*) *Trans*-tethering using soluble C2AB domains is only observed at higher C2AB concentrations when the surfaces of the liposomes are already saturated by *cis*-binding. (*D*) At lower concentrations of soluble C2AB domains only *cis*-binding but no tethering can be observed. (*E*) Synaptotagmin-1 can tether acceptor vesicles by binding to syntaxin as well as to binary and ternary SNARE complexes in the absence of acidic phospholipids. (*F*) However, also in this case *cis*-binding dominates over *trans*-tethering if the donor membrane contains acidic phospholipids.

was only observed when both C2 domains were intact or when 1% PiP_2 was present in the target membrane. Evidently, membrane anchorage does not interfere with the ability of the C2 domains to interact *in trans*. Similarly, binding is also observable to membrane-anchored SNAREs, which is (with the exception of binding to isolated syntaxin) not significantly enhanced by calcium, again in agreement with previous studies (1, 5–7). In contrast, all *trans* interactions were completely abolished when *cis* binding was enabled by inclusion of 12 or 20% acidic phospholipids (PS) in the resident membrane of synaptotagmin.

This finding is surprising because several previous studies (10, 17, 27) have shown that soluble fragments containing both C2 domains or even only the C2B domain are capable of clustering vesicles. Obviously, clustering can only occur as long at least two independent binding sites are present. Although we have confirmed this notion, our data show that clustering induced by soluble C2AB domains is only observable when concentrations are used under which binding is saturating, which seems to be the case in most studies. At limiting concentrations soluble C2AB is only capable of interacting with the same membrane. Why membrane cross-linking is only observable under saturating conditions is not clear. If binding sites are limited (as under saturating conditions) the membrane of all liposomes will be similarly crowded. However, *cis*-binding may be retarded because probably more area is required to position both C2 domains of the same C2AB in the correct orientation on one membrane, whereas less space may still suffice to bind two C2 domains of two different C2AB parallel *in trans*. Alternatively, it is conceivable that C2AB molecules are capable of *trans*-interactions that are only sufficiently strong for tethering if the membrane is completely covered with them. We believe that many of the seemingly contradictory findings in the literature (10, 22) can thus be reconciled. In particular, our results confirm and extend previous observations in which reduced fusion efficiency in liposome experiments involving synaptotagmin-1 was attributed to *cis*-binding of the C2 domains (24, 27), and they may explain some of the conflicting data on synaptotagmin-1 action on fusion in artificial systems (24, 25, 27). While this work was in progress, it was reported that fusion between SNARE and synaptotagmin-containing liposomes in vitro is only stimulated by Ca^{2+} if there is excess PS in the acceptor membrane, nicely complementing the findings reported in our study (28). Also, after submission of this manuscript, similar results have been published (29) based on a similar experimental approach as described in Cypionka et al. (23), which largely agrees with the data presented here.

More importantly, the results raise interesting questions concerning the function of *cis*- vs. *trans*-interactions of synaptotagmin in the synapse. Synaptic vesicles contain more than 15% anionic phospholipids suggesting that *cis*-binding may occur under physiological conditions unless prevented by other factors such as charge screening and molecular crowding. On the other hand, in a docked vesicle both the vesicle and the plasma membrane may be sufficiently close to compensate for the preference of *cis*-binding, thus allowing cross-linking via the C2 domains, with one of them binding to the plasma membrane and the other one to the vesicle membrane (*cis-trans*) as previously suggested (17, 25). It remains to be clarified whether synaptotagmins action in exocytosis requires such calcium-dependent cross-linking of the C2 domains or whether *trans*-binding of the C2 domains is sufficient while the protein remains anchored to the vesicle by its transmembrane domain. Also, two recent single-liposome microscopy studies suggested that synaptotagmin-1 massively enhanced membrane fusion even without substantial tethering of the membranes. In these studies tethering was mediated by SNARES (24, 25) (Fig. 4). Finally, it cannot be excluded (although we consider it as unlikely) that calcium-dependent *cis*-binding suffices to trigger exocytosis, for instance, by inducing curvature in the vesicle membrane. In any case, membrane tethering by synaptotagmin probably comprises a subtle balance of competing *cis*- and *trans*-interactions, which may be modulated by other factors, adding yet another potential mechanism for modulating synaptotagmin-stimulated exocytosis in the synapse.

Methods

Synaptotagmin-1 and SNAREs (rat sequences, bacterial expressed) were purified as described (3, 27). All lipids [phosphatidylcholine (PC), phosphatidylethanolamine (PE), phosphatidylserine (PS), cholesterol, phosphatidylinositol-4,5-bisphosphate (PiP_2)] were purchased from Avanti Polar Lipids except for the Texas Red-labeled phosphatidylethanolamine (TRPE) and Oregon Green-labeled phosphatidylethanolamine (OGPE), which were purchased from Invitrogen. Lipid mixtures with either 0 mol%, 5 mol%, 12 mol %, or 20 mol% PS, 20% PE (including 1% TRPE or 1.5% OGPE), 10% cholesterol, 0 or 1% PiP_2, and PC stocks were first prepared by resolving lipid films in 5% sodium cholate HP buffer (20 mM Hepes, 150 nM KCl, 2 mM DTT, 5% sodium cholate, pH 7.4). The final concentration of the lipids was 27 mM. To 16.7 μL of the lipid mixtures, protein was added to achieve a protein:lipid ratio of 1:1,000, except the synaptotagmin-SNAREs experiments (here the synaptotagmin to lipid ratio was 1:750). The lipid protein mixes were filled with 1.5% sodium cholate HP buffer to a final volume of 50 μL. The liposomes were formed by detergent removal using a Sephadex G50 superfine column (Sigma; Bio-Rad). The running buffer for the column was HP150 buffer (20 mM Hepes, 150 nM KCl, 2 mM DTT, pH 7.4). The size of liposomes was about 50 nm. The two-photon confocal microscope has been described in ref. 23, except that we used an UPlanSApo 60× NA 1.2 water immersion objective (Olympus). Membrane tethering was measured at 20 °C by FCCS as described (23) and immediately after mixing 10 nM of each liposome population (approximately 0.09 mg/mL each color) in 20 mM Hepes pH 7.5, 150 mM KCl, 2 mM DTT, 1 mM EGTA with or without 1.1 mM $CaCl_2$ for 100 μM Ca^{2+}. The data presented in Figs. 1–4 and Figs. S2*A* and S3 represent mean values of at least two independent experiments (bar indicates range of data points) with each experiment representing the average of at least five technical replicates. The Ca^{2+} titration curves presented in Fig. S2*B* represent mean values of at least five technical replicates (each of 10 s measuring time) of a single sample batch. The error in the technical replicates was ~10–20%. More details on the sample preparation as well as FCS analysis can be found in *SI Methods*.

ACKNOWLEDGMENTS. We thank Pen-Nan Liao for his extensive help in preparing the figures and Jian-Hua Chen for his help in measuring liposome tethering. G.v.d.B. is the recipient of a fellowship from the Human Frontier Science Program. This work was supported by National Institutes of Health Grant P01GM072694 (to R.J.) and the Deutsche Forschungsgemeinschaft SFB803 (to W.V., M.G., R.J., and P.J.W.).

1. Chapman ER (2008) How does synaptotagmin trigger neurotransmitter release? *Annu Rev Biochem* 77:615–641.
2. Martens S, McMahon HT (2008) Mechanisms of membrane fusion: Disparate players and common principles. *Nat Rev Mol Cell Biol* 9:543–556.
3. Radhakrishnan A, Stein A, Jahn R, Fasshauer D (2009) The Ca^{2+} affinity of synaptotagmin 1 is markedly increased by a specific interaction of its C2B domain with phosphatidylinositol 4,5-bisphosphate. *J Biol Chem* 284:25749–25760.
4. Fernandez I, et al. (2001) Three-dimensional structure of the synaptotagmin 1 C2B-domain: 1 as a phospholipid binding machine. *Neuron*, 32:1057–1069, Synaptotagmin.
5. Bai J, Wang CT, Richards DA, Jackson MB, Chapman ER (2004) Fusion pore dynamics are regulated by synaptotagmin*t-SNARE interactions. *Neuron* 41: 929–942.
6. Vrljic M, et al. (2010) Molecular mechanism of the synaptotagmin-SNARE interaction in Ca^{2+}-triggered vesicle fusion. *Nat Struct Mol Biol* 17:325–331.
7. Choi UB, et al. (2010) Single-molecule FRET-derived model of the synaptotagmin 1-SNARE fusion complex. *Nat Struct Mol Biol* 17:318–324.
8. Li L, et al. (2006) Phosphatidylinositol phosphates as co-activators of Ca^{2+} binding to C2 domains of synaptotagmin 1. *J Biol Chem* 281:15845–15852.
9. Bai J, Tucker WC, Chapman ER (2004) PIP2 increases the speed of response of synaptotagmin and steers its membrane-penetration activity toward the plasma membrane. *Nat Struct Mol Biol* 11:36–44.
10. Araç D, et al. (2006) Close membrane-membrane proximity induced by $Ca^{(2+)}$-dependent multivalent binding of synaptotagmin-1 to phospholipids. *Nat Struct Mol Biol* 13:209–217.

11. Gaffaney JD, Dunning FM, Wang Z, Hui E, Chapman ER (2008) Synaptotagmin C2B domain regulates Ca^{2+}-triggered fusion in vitro: critical residues revealed by scanning alanine mutagenesis. *J Biol Chem* 283:31763–31775.
12. Bhalla A, Chicka MC, Tucker WC, Chapman ER (2006) $Ca(^{2+})$-synaptotagmin directly regulates t-SNARE function during reconstituted membrane fusion. *Nat Struct Mol Biol* 13:323–330.
13. Herrick DZ, Sterbling S, Rasch KA, Hinderliter A, Cafiso DS (2006) Position of synaptotagmin I at the membrane interface: Cooperative interactions of tandem C2 domains. *Biochemistry* 45:9668–9674.
14. Hui E, Bai J, Chapman ER (2006) Ca^{2+}-triggered simultaneous membrane penetration of the tandem C2-domains of synaptotagmin I. *Biophys J* 91:1767–1777.
15. Schiavo G, Gu QM, Prestwich GD, Söllner TH, Rothman JE (1996) Calcium-dependent switching of the specificity of phosphoinositide binding to synaptotagmin. *Proc Natl Acad Sci USA* 93:13327–13332.
16. Xue M, et al. (2008) The janus-faced nature of the C_2B domain is fundamental for synaptotagmin-1 function. *Nat Rev Mol Cell Biol* 15:1160–1168.
17. van den Bogaart G, et al. (2011) Synaptotagmin-1 may be a distance regulator acting upstream of SNARE nucleation. *Nat Struct Mol Biol* 18:805–812.
18. Rhee JS, et al. (2005) Augmenting neurotransmitter release by enhancing the apparent Ca2+ affinity of synaptotagmin 1. *Proc Natl Acad Sci USA* 102:18664–18669.
19. Martens S, Kozlov MM, McMahon HT (2007) How synaptotagmin promotes membrane fusion. *Science* 316:1205–1208.
20. McMahon HT, Kozlov MM, Martens S (2010) Membrane curvature in synaptic vesicle fusion and beyond. *Cell* 140:601–605.
21. Hui E, Johnson CP, Yao J, Dunning FM, Chapman ER (2009) Synaptotagmin-mediated bending of the target membrane is a critical step in $Ca(^{2+})$-regulated fusion. *Cell* 138: 709–721.
22. Hui E, et al. (2011) Mechanism and function of synaptotagmin-mediated membrane apposition. *Nat Struct Mol Biol* 18:813–821.
23. Cypionka A, et al. (2009) Discrimination between docking and fusion of liposomes reconstituted with neuronal SNARE-proteins using FCS. *Proc Natl Acad Sci USA* 106: 18575–18580.
24. Lee HK, et al. (2010) Dynamic Ca^{2+}-dependent stimulation of vesicle fusion by membrane-anchored synaptotagmin 1. *Science* 328:760–763.
25. Kyoung M, et al. (2011) In vitro system capable of differentiating fast Ca^{2+}-triggered content mixing from lipid exchange for mechanistic studies of neurotransmitter release. *Proc Natl Acad Sci USA* 108:E304–E313.
26. Haustein E, Schwille P (2007) Fluorescence correlation spectroscopy: Novel variations of an established technique. *Annu Rev Biophys Biomol Struct* 36:151–169.
27. Stein A, Radhakrishnan A, Riedel D, Fasshauer D, Jahn R (2007) Synaptotagmin activates membrane fusion through a Ca^{2+}-dependent *trans* interaction with phospholipids. *Nat Struct Mol Biol* 14:904–911.
28. Lai Y, Shin YK (2012) The importance of an asymmetric distribution of acidic lipids for synaptotagmin 1 function as a Ca^{2+} sensor. *Biochem J* 443:223–229.
29. Kim J-Y, et al. (2012) Solution single-vesicle assay reveals PIP(2)-mediated sequential actions of synaptotagmin-1 on SNAREs. *EMBO J* 31:2144–2155.

Supporting Information

Vennekate et al. 10.1073/pnas.1116326109

SI Methods

Protein Constructs. The protein constructs were from *Rattus norvegicus*. They were cloned into the expression vector pET28a. Expression constructs of the full-length protein (amino acids 1–421) and of the soluble domain of synaptotagmin (amino acids 97–421), have been described before (1). In the same publications, the calcium mutants of the full-length protein have also been described (1): C2a*B (D178A, D230A, and D232A), C2Ab* (D309A, D363A, and D365A), C2a*b* (D178A, D230A, D232A, D309A, D363A, and D365A), and KAKA mutant (K326A and K327A). The constructs for the neuronal SNAREs were the SNARE motif of syntaxin 1A with its *trans*-membrane domain (amino acids 183–288), a cysteine-free variant of SNAP-25A (amino acids 1–206), and synaptobrevin 2 without its *trans*-membrane domain (amino acids 1–96). The synaptotagmin 1 (amino acids 97–421) single cysteine variant (S342C) was obtained after first removing the single native cysteine (C278S) and then introducing a point mutation at position 342 (1, 2).

Protein Purification and Labeling. All proteins were expressed in *Escherichia coli* strain BL21 (DE3) and purified using Ni^{2+}-nitrilotriacetic acid beads (GE Healthcare), followed by further purification using ion exchange chromatography as described (1) with a few modifications. The protein concentrations were determined by a Bradford assay or UV absorption (2). Labeling of the synaptotagmin-1 (amino acids 97–421) single cysteine variant (S342C) with Alexa Fluor 488 C_5 maleimide was done as follows. First the proteins were dialyzed against the labeling buffer (50 mm Hepes, pH 7.4, 500 mm NaCl, 100 μm Tris(2-carboxyethyl) phosphine). The dialyzed protein solution was incubated with the fluorophore for 2 h at room temperature. Thereafter, the labeled protein was separated from the unreacted dye using a Sephadex G50 superfine column. The labeling efficiency was ∼40%. Syntaxin 1A (183–288) and synaptobrevin 2 (1–96) were purified by ion-exchange chromatography (2) in the presence of 15 mm CHAPS. The binary complex containing syntaxin 1A (183–288) and SNAP-25A was assembled from purified monomers and subsequently purified by ion-exchange chromatography in the presence of 1% CHAPS (2). The ternary SNARE complex syntaxin 1A (183–288), SNAP-25A, and synaptobrevin 2 (1–96) was generated by incubation of the binary complex and synaptobrevin 2 (1–96) in a ratio of 1:2 overnight at 4 °C. The excess synaptobrevin 2 was removed with Sephadex G50 superfine column during liposome reconstitution. Full-length synaptotagmin was purified in the presence of 1% CHAPS using ion exchange chromatography (as described in ref. 2).

Liposome Reconstitution. All lipids were purchased from Avanti Polar Lipids except for the Texas Red-labeled phosphatidylethanolamine (TRPE) and Oregon Green-labeled phosphatidylethanolamine (OGPE), which were purchased from Invitrogen. Lipid mixtures according to Table S1 were first prepared by resolving lipid films in HP buffer (20 mM Hepes, 150 nM KCl, 2 mM DTT, pH 7.4) containing 5 % sodium cholate (mass fraction). The final concentration of the lipids was 27 mM. To 16.7 μL of the lipid mixtures protein was added to achieve a protein:lipid ratio of 1:1,000, expect the synaptotagmin-SNAREs experiments (here the synaptotagmin-to-lipid ratio was 1:750). The lipid protein mixtures were adjusted with HP buffer containing 1.5% sodium cholate (mass fraction) to a final volume of 50 μL. The liposomes were formed by detergent removal using a Sephadex G50 superfine column (Sigma; Bio-Rad). The running buffer for the column was HP150 buffer (20 mM Hepes, 150 nM KCl, 2 mM DTT, pH 7.4). The collected liposome volume was about 250 μL. The size of liposomes was about 50 nm. For all liposomes used in this study the average lipid number per liposome was ∼12,000. Also, in all experiments the liposome concentration was 10 nM liposomes corresponding to a lipid concentration of 0.09 mg/mL for each type of colored liposomes [based on liposome sizes (3) and space required for lipids (4)]. In Table S1, the composition of the liposomes for all data shown in Figs. 1–4 and Figs. S2 and S3 are shown.

Fluorescence Cross-Correlation Spectroscopy (FCCS) Setup. For simultaneous two-photon excitation of differently labelled liposomes we used a titanium-sapphire laser (800 nm, 87 MHz, Fig. S1*A*). The laser beam was expanded using a lens system and coupled with a dichroic mirror (715 DSCPXR; AHF) into a UPlanSApo 60×/1.2-W water immersion objective (Olympus). The emitted photons passed through the objective and the dichroic mirror. Scattered light from excitation beam was blocked by a short pass filter (E700SP2; AHF). The emission was collimated using a second lens system, separated by a second dichroic mirror (590 DCXR; AHF), filtered in each direction with a band pass filter (HQ 645/75 and HQ 535/50; AHF) and collected by separate avalanche photodiodes (APD) (SPCM-AQR-13; PerkinElmer). The transistor–transistor logic (TTL) signals from the APD were analyzed using a four-channel router (PRT 400; PicoQuant) and a time-correlated single photon counting (TCSPC) card (TimeHarp200; PicoQuant) and saved in time-tagged time-resolved (TTTR) format. The correlation was processed using a homemade program.

For the measurements without or with 100 μM Ca^{2+} either the buffer containing 20 mM Hepes, 150 mM potassium chloride, 1 mM EGTA or the buffer containing 20 mM Hepes, 150 mM potassium chloride, 1 mM EGTA, 1.1 mM calcium chloride was used. The reaction volume was 100 μL. The measurement was started by diluting the red and green liposome stock solutions into the corresponding reaction buffer and loading a droplet (20 μL) onto the coverslip after short vortexing. The final concentration of the liposomes was ∼10 nM for each color (corresponding to ∼0.09 mg/mL lipids). The signal traces for the TP-FCCS analysis were recorded six times for 12 seconds for each droplet resulting in a total measuring time of 72 seconds per droplet. This procedure was repeated several times with different droplets from the same solution. Each experiment using different liposome protein and lipid compositions as well as Ca^{2+} concentrations was repeated at least one time with fresh liposome and buffer preparations.

Tethering Assay and Binding of Labeled, Soluble C2AB-Fragments. The tethering assay has been described in detail (3). In general, the average number of particles in the focal detection volume that carry Oregon Green-labeled lipids, N_g, can be calculated from the inverse of the autocorrelation amplitude for the Oregon Green fluorescence $N_g = G_g(0)^{-1}$ at small lag times (green line in Fig. S1*B*). Here, a particle can be either a single liposome or a particle consisting of two or more tethered liposomes for which at least one liposome also contains Oregon Green-labeled lipids. Under our experimental conditions, the influence of different liposome/particle compositions on N_g can be neglected (3). In the same manner the average particle number for Texas Red-labeled particles, N_r, can be calculated from the inverse of the autocorrelation amplitude for the Texas

Red fluorescence N_r, = $G_r(0)^{-1}$ at small lag times (red line in Fig. S1*B*). The average particle number in the focal detection volume that carries both types of labeled lipids, N_{rg}, was calculated from the particle numbers N_g and N_r and the cross-correlation amplitude for the Texas Red and Oregon Green fluorescence (blue line in Fig. S1*B*) at small lag times: $N_{rg} = G_{rg}(0)\cdot N_g\cdot N_r$. By comparing this number of double-labeled particles, N_{rg}, with the total number of particles carrying green labels, N_g, the tethering percentage can be calculated: Tethering (%) = $N_{rg}/N_g \cdot 100$. Only in the case of Fig. 3*A* this percentage was calculated by $N_{rg}/N_r\cdot 100$ because here the number of green-labeled C2AB fragment was present in large excess in most cases in comparison with the number of red liposomes. Therefore, the tethering percentage $N_{rg}/N_r\cdot 100$ represents the percentage of liposomes carrying significant amounts of C2AB fragments in comparison with the total amount of liposomes. On the contrary, the $N_{rg}/N_g\cdot 100$ used for Fig. 3*B* represents the amount of C2AB fragment attached to liposomes. In this case only relative extents in C2AB fragments binding can be given at higher percentages of bound C2AB, because a liposome carrying many green C2AB fragments is a lot brighter than a single-labeled C2AB fragment. However, even though only relative bound fractions can be exactly concluded from the analysis shown in Fig. 3*B* it provides clear evidence that at 215 nM C2AB a significantly smaller fraction of C2AB is bound to the membranes than at 50 nM C2AB. This can only be explained by a saturation of the membranes. Because full tethering is still not observed at 860 nM soluble C2AB (Fig. 2), this provides evidence that clustering occurs at saturating concentrations.

1. Stein A, Radhakrishnan A, Riedel D, Fasshauer D, Jahn R (2007) Synaptotagmin activates membrane fusion through a Ca^{2+}-dependent *trans* interaction with phospholipids. *Nat Struct Mol Biol* 14:904–911.
2. Radhakrishnan A, Stein A, Jahn R, Fasshauer D (2009) The Ca^{2+} affinity of synaptotagmin 1 is markedly increased by a specific interaction of its C2B domain with phosphatidylinositol 4,5-bisphosphate. *J Biol Chem* 284:25749–25760.
3. Cypionka A, et al. (2009) Discrimination between docking and fusion of liposomes reconstituted with neuronal SNARE-proteins using FCS. *Proc Natl Acad Sci USA* 106: 18575–18580.
4. Nagle JF, Tristram-Nagle S (2000) Structure of lipid bilayers. *Biochim Biophys Acta* 1469: 159–195.

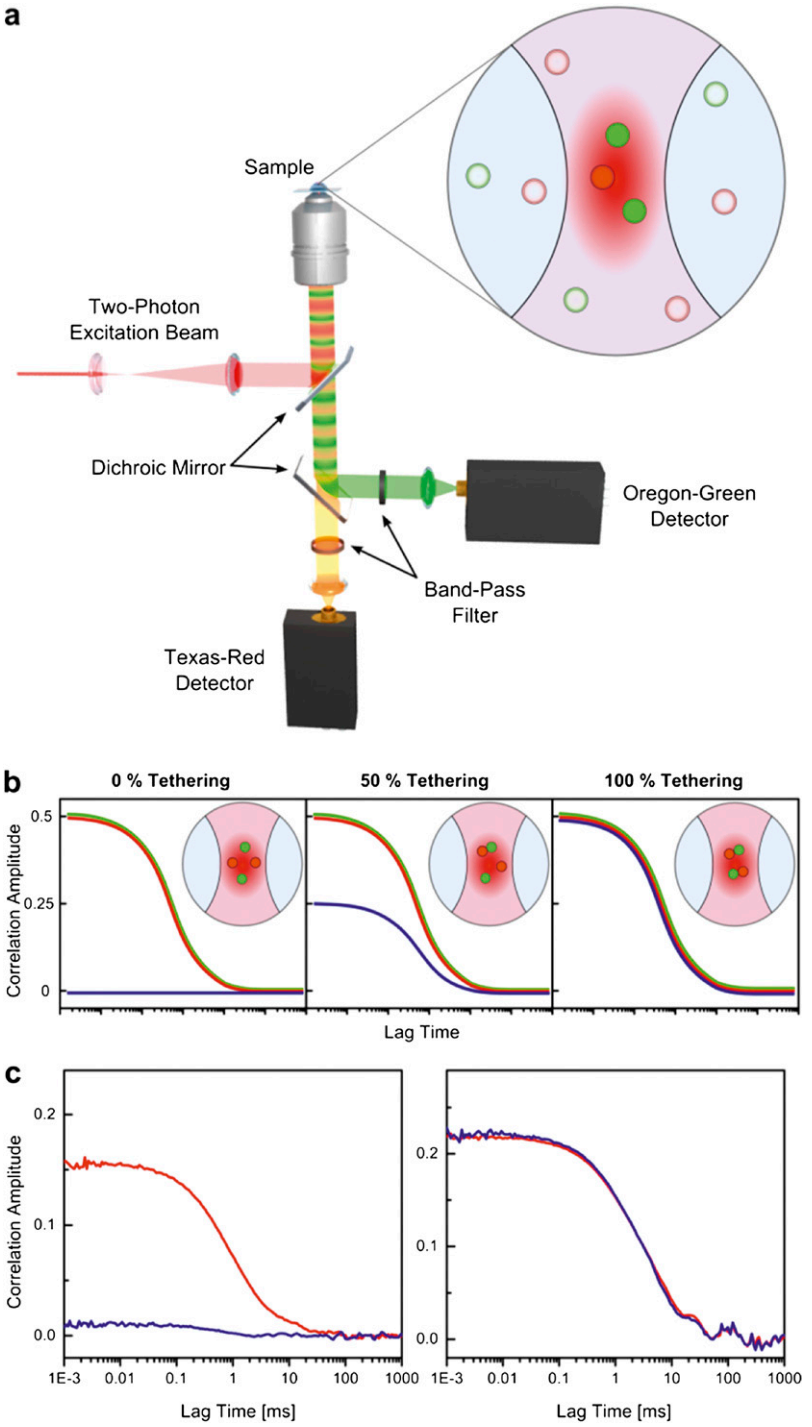

Fig. S1. TP-FCCS tethering assay. (*A*) In the TP-FCCS set-up fluorescence fluctuations caused by diffusion of labeled liposomes through the microscopic two-photon excitation volume (dimensions ~200–500 nm) are recorded and analyzed by correlation functions. (*B*) Schematic presentation of the correlation functions. Amplitudes of the red or green auto-correlation curves (correspondingly colored curves) are inversely proportional to the average number of red- or green-labeled liposomes in the detection volume, respectively. For example, the amplitudes of 0.5 of the red and green curves reflect approximately two red- or green-labeled particles that are on average in the excitation volume. Cross-correlation amplitude (blue) relative to the autocorrelation amplitudes is a direct measure for the proportion of tethered red-green liposomes in the total liposome population. (*C*) Exemplary measured autocorrelation curve of Texas-Red labeled, synaptotagmin-containing vesicles (red) and of the cross-correlation (blue) with Oregon-Green–labeled liposomes. *Left*, no or little tethering with an inactive mutant of synaptotagmin-1 (D178A D230A D232A D309A K325A K326A D363A D365A). *Right*, 100% tethering by wild-type synaptotagmin-1. For more details see ref. 1.

1. Cypionka A, et al. (2009) Discrimination between docking and fusion of liposomes reconstituted with neuronal SNARE-proteins using FCS. *Proc Natl Acad Sci USA* 106: 18575–18580.

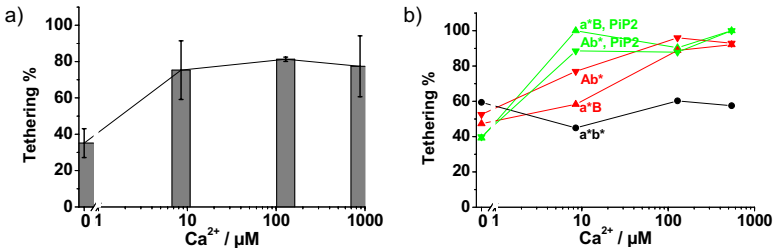

Fig. S2. Tethering of liposomes mediated by membrane-bound synaptotagmin-1. Dependence on the Ca^{2+} concentration and on the presence of PiP_2 in the target membrane. Tethering was measured as in Fig. 1. (*A*) Ca^{2+}-concentration dependence of membrane tethering by wild-type synaptotagmin in the absence of PiP_2 in the target membrane. (*B*) Ca^{2+}-titration curves of synaptotagmin mutants. At Ca^{2+} concentrations of about ~8.5 μM the tethering for both, C2A*b* and C2a*B*, is lower than at ~100 μM (red curves) but in the presence of 1 mol% PiP_2 in the target membrane full tethering is observed (green curves). In contrast to wild-type synaptotagmin, no significant increase of tethering with increasing Ca^{2+} concentrations can be observed for the double mutant a*b* (black curve). See Fig. 1 legend for an explanation of the synaptotagmin variants.

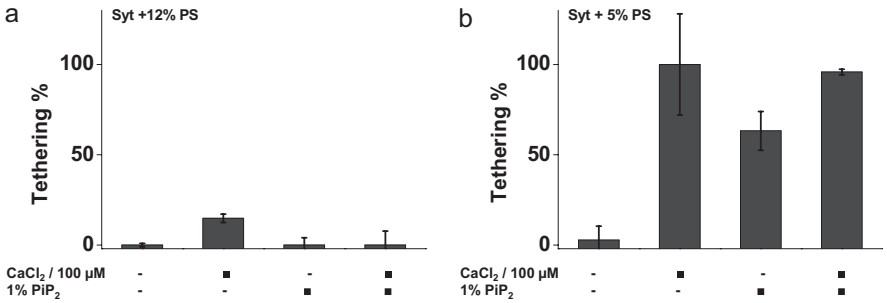

Fig. S3. Membrane tethering by synaptotagmin in the presence of 5 and 12% PS in the synaptotagmin-containing membrane. (*A*) Presence of 12% PS prevented membrane tethering in a very similar fashion as 20% PS (Fig. 1), regardless of whether the target membrane contains PS only or PS plus PiP_2. (*B*) A total of 5% PS is not sufficient anymore to inhibit the activity of synaptotagmin-1 by *cis*-binding if either 100 μM Ca^{2+} is present in the solution or 1% PiP_2 in the target membrane. Only the absence of both allows an inactivation of synaptotagmin tethering by the presence of 5% PS in the synaptotagmin-1–containing membranes.

Table S1. Percentages of lipid composition

	PC	PE	TRPE	OGPE	PS	Chol	PiP_2
Fig. 1*A*, red	70	19	1	0	0	10	0
Fig. 1*A*, green	50	18.5	0	1.5	20	10	0
Fig. 1*B*, red	70	19	1	0	0	10	0
Fig. 1*B*, green	49	18.5	0	1.5	20	10	1
Fig. 1*C*, red	50	19	1	0	20	10	0
Fig. 1*C*, green	50	18.5	0	1.5	20	10	0
Fig. 1*D*, red	50	19	1	0	20	10	0
Fig. 1*D*, green	49	18.5	0	1.5	20	10	1
Fig. 2, red	50	19	1	0	20	10	0
Fig. 2, green	50	18.5	0	1.5	20	10	0
Fig. 3 *A* and *B*, red	50	19	1	0	20	10	0
Fig. 4 *A*, *B*, and *D*, red	70	19	1	0	0	10	0
Fig. 4, all green	70	18.5	0	1.5	0	10	0
Fig. 4 *C* and *E*, red	50	19	1	0	20	10	0
Fig. S2*A*	70	19	1	0	0	10	0
Fig. S2*B*, black and red	70	19	1	0	0	10	0
Fig. S3, green	49	18.5	0	1.5	20	10	1
Fig. S3*A*, red	65	19	1	0	5	10	0
Fig. S3*B*, red	58	19	1	0	12	10	0
Fig. S3 *A* and *B*, green	50	18.5	0	1.5	20	10	0
Fig. S3 *A* and *B*, green	49	18.5	0	1.5	20	10	1

Chol, cholesterol; OGPE, Oregon green phosphatidylethanolamine; PC, phosphatidylcholine; PE, phosphatidylethanolamine; PIP_2, phosphatidylinositol 4,5-bisphosphate; PS, phosphatidylserine; TRPE, Texas red phosphatidylethanolamine.